Nuclear Engineering and Design 389 (2022) 111648

Contents lists available at ScienceDirect

Nuclear Engineering and Design

journal homepage: www.elsevier.com/locate/nucengdes

Implications of HALEU fuel on the design of SMRs and micro-reactors

Liam Carlson [1], James Miller, Zeyun Wu *

Department of Mechanical and Nuclear Engineering, Virginia Commonwealth University, 401 W. Main St., Richmond, VA 23219, USA

ABSTRACT

Since the construction of the first commercial nuclear power plant in 1957, the nuclear power industry has operated under the philosophy of economy of scale - the idea that increased power plant size accounts for higher economic efficiency. However, there has been a recent shift in direction; small modular reactors (SMRs) and micro-reactors are being considered as potentially wise investments for commercial power producers in that they can provide advantages that large-scale reactors may not possess in terms of reactor safety and investment risk. However, this may come at the risk of a higher levelized cost of electricity (LCOE). LCOE may be reduced by enriching the fuel passed its regulated limit of 5 wt% (w/o) ^{235}U. The high assay low-enriched uranium (HALEU) fuel (5–20 w/o ^{235}U) is introduced to increase the plant capacity factor, which thereby decrease fuel supply costs and reduce the LCOE. While decreasing plant LCOE seems like a clear advantage, several issues may result from increasing enrichments to the HALEU level in an SMR or micro-reactor design. This paper aims to shed light on these issues and address how they may affect the overall reactor design by using HALEU fuels in these reactors.

This paper first discusses the notable effects on a reactor design with higher enrichment, then analyzes a SMR case study based on the NuScale's 160 MWth SMR design. The case study reveals that the SMR with higher enriched fuel was able to double both fuel burnup and cycle time with an average core enrichment of 8.34 w/o and a maximum average assembly enrichment of 9.10 w/o. Moreover, this higher enriched core was found to operate with a maximum global peaking factor of 1.86, well below the published limit of 2.0. Likewise, the maximum axial flux offset of −2.4% and the maximum boron concentration of 1757 ppm both remain within their respective safety constraints. Notable fission poisons, such as ^{149}Sm and ^{135}Xe, were also found to sharply increase in the HALEU core. Additionally, the average fuel temperature and peak cladding temperature fell within their respective safety constraints. Core-averaged flux, fluence, cladding creep, and post-shutdown decay heat were also investigated. Lastly, the higher enriched core was found to reduce LCOE by approximately 1.23 $/MWh.

1. Introduction

1.1. Current status of SMR and Micro-reactor designs

Small modular reactors (SMRs) and micro-reactors are commercial nuclear reactor designs that produce less power than conventional large reactors such as the large scale pressurized water reactors (PWRs). SMRs range up to 300 MWe and are comprised of factory manufactured parts and components (Kirshenberg, et al., 2017). Micro-reactors (also known as very small reactors) operate under 15 MWe and are transportable as an entire unit (Wna, 2020). Proposed micro-reactor utilization would be in the powering of small remote communities or providing on-site power for military purposes (McGinnis, 2019; Charles, 2018). Most of the United States nuclear reactor fleet is comprised of large reactors, those rated at 700 MWe or greater. Medium reactors operate between 300 and 700 MWe and are not considered to be cost-effective because they do not take advantage of economy of scale, nor can they utilize the design advantages possible for SMRs and micro-reactors (Locatelli et al., 2014).

SMRs and micro-reactors have several advantages that make them competitive with large-scale reactors. The most obvious advantages are modularity and reduced capital cost (one-time costs required for plant operation such as land, construction, and equipment). Naturally, small power plants of any kind require smaller capital investments. The low capital cost of a small power plants allows for shorter payback periods and lower financial risk (Locatelli et al., 2014). This reduction in upfront investment may encourage small nations and utilities to invest in commercial nuclear power production. On the other hand, distributing the energy production equivalent of a single larger reactor between multiple small power plants of similar design nullifies the economy of scale advantage of the former, resulting in a higher cost per unit energy production. The increase in higher levelized cost of electricity (LCOE) may make small-scale power plants seem like a worse long-term investment when compared to large power plants; however, SMRs and micro-reactors may be beneficial for those cases where only small to medium additions to a power grid or community are needed (Locatelli et al., 2014). With a greater possibility of being sited closer to their customers, SMRs and micro-reactors benefit from less of a demand for power transmission infrastructure. They are able to be built on sites not

* Corresponding author.
E-mail address: zwu@vcu.edu (Z. Wu).
[1] Current address: Department of Nuclear Engineering, Texas A&M University, College Station, TX 77843, USA.

https://doi.org/10.1016/j.nucengdes.2022.111648
Received 4 September 2021; Received in revised form 21 December 2021; Accepted 6 January 2022
Available online 13 January 2022

possible for conventional large nuclear power plants (Kirshenberg, et al., 2017), and micro-reactors offer an economic advantage for small communities which rely on relatively expensive diesel generators (Prasad et al., 2015).

Additionally, some SMRs have drastically different designs than traditional light water reactors (LWRs). These unique SMR designs including gas-cooled and liquid metal coolant reactors are designed with relatively high capacity factors. Some SMR designs, such as the high-temperature reactor-pebble bed module (HTR-PM), may be refueled continuously throughout its lifetime. This advantage is offset to some extent by the design's greater security and safety issues (Prasad et al., 2015; Moormann et al., 2018). Despite an HTR-PM type reactor currently under construction in China, the U.S. is unlikely to license and deploy these high-concept SMR designs in the near future.

While SMRs and micro-reactors do not benefit from the economy of scale, they do have unique capabilities that separate these designs from traditional large reactors. Most prominently, the factory-produced modular parts of SMRs and micro-reactors lower the levelized capital and operation and maintenance (O&M) costs. It is worth mentioning, however, that some newer large reactor designs, such as the AP1000 may also take advantage of modular construction techniques. Standardized parts allow components to be mass-produced and more cheaply replaced. Additionally, the distributed load of many small power plants, as opposed to one large power plant, reduces the risk of power outage in the case of a plant unexpectedly going offline. SMRs can operate with longer cycles and are expected to have shorter refueling times. Since smaller reactors operate at lower thermal power, it takes much less time to reduce post-shutdown decay heat than their large reactor counterparts. This increase in capacity factor reduces the burden of other power plants to carry the load as an SMR or micro-reactor is taken offline or is operating below full-power conditions. SMRs also benefit from enhanced safety due to lower thermal power and passive safety systems like natural circulation (McGinnis, 2019). SMRs and micro-reactors may also be ideal candidates to perform secondary functions such as medical isotope production and ocean water desalination.

Despite these advantages, SMRs and micro-reactors suffer a number of disadvantages compared to large reactors. For one, small-scale reactors introduce increased concerns regarding the proliferation of nuclear material. Since the implementation of SMRs is expected to increase the number of nuclear sites needed to produce the same power as a large plant, the risk of security-related incidents is likely to increase. Additionally, the location of SMRs and micro-reactors in remote communities and developing nations also results in added stress on the nuclear security infrastructure (Prasad et al., 2015). There are also several design issues that reduce the effectiveness of SMRs and micro-reactors. For example, smaller reactor cores suffer from increased fast neutron leakage (Wade and Fujita, 1989). This is one reason why SMRs and micro-reactors rely on higher enriched fuel to sustain criticality. Additionally, smaller active fuel heights reduce overall heat transfer within the core, thereby reducing the reactor's thermal efficiency. Overall, commercial SMRs and micro-reactors are first of a kind, meaning there is a relatively low amount of empirical data from which to evaluate design concepts before implementation. Thus, there is a lengthy and expensive licensing and review process, even for those designs with the least deviation from present LWR designs.

For many experts, the potential benefits of these reactors are judged to outweigh the disadvantages enough to justify developing SMRs and micro-reactors for commercial use. Some companies such as NuScale and Oklo are currently pursuing small reactor development. NuScale is currently under licensing review with the NRC for the construction and operation of a power station consisting of up to twelve 160MWt light-water SMRs (U.S. NRC., 2012). In March 2020; Oklo applied to the NRC to develop a 4.5 MWt compact fast micro-reactor based on the EBR-II design. Additionally, there are currently many other operational modular or non-modular small reactor concepts proposed in The U.S. and worldwide. Table 1 summarizes project status of a selection of SMR and micro-reactor projects with wide variations in power level, reactor type, and nationality (Wna, 2020). It is evident there exists a sizable amount of interest in SMR and micro-reactor power production for commercial distribution.

Table 1
SMR and Micro-reactor Projects (Wna, 2020).

Reactor	Capacity	Type	Developer	Nation	Project Status
CAREM-25	27 MWe	Integral PWR	CNEA & INVAP	Argentina	Under Construction
HTR-PM	210 MWe	Twin HTR[1]	INET, CNEC & Huaneng	China	Under Construction
NuScale	45 MWe	Integral PWR	NuScale Power	USA	Near-Term Deployment
BWRX-300	300 MWe	BWR[2]	GE Hitachi	USA	Near-Term Deployment
Integral MSR	192 MWe	MSR[3]	Terrestrial Energy	Canada	Near-Term Deployment
RITM-200M	50 MWe	Integral PWR	OKBM	Russia	Near-Term Deployment
mPower	195 MWe	Integral PWR	BWXT	USA	Shelved
PBMR	165 MWe	HTR	HTMR Ltd	South Africa	Shelved
Xe-100	75 MWe	HTR	X-energy	USA	Early Stages
Leadir-PS100	36 MWe	Lead-cooled	Northern Nuclear	Canada	Early Stages
Aurora	1.5 MWe	Heat pipe FNR[4]	Oklo	USA	Early Stages
Sealer	3–10 MWe	Lead FNR	LeadCold	Sweden	Early Stages

[1] High temperature reactor
[2] Boiling water reactor
[3] Molten salt reactor
[4] Fast-neutron reactor

1.2. HALEU fuels

One method for improving the economic efficiency of SMRs and micro-reactors is to extend the cycle length by increasing fuel burnup. In order to do this, reactors must utilize fuels above the current NRC limit of 5 w/o enrichment. These fuels, known as high assay low-enriched uranium (HALEU) fuels, are of high interest to utilities for their ability to reduce overall plant costs, which is why research institutions and industry are working with the NRC to change standards to include HALEU level enrichments. Because they contain more fissile material, HALEU implementation can increase the capacity factor and reduce the fuel costs of a reactor by increasing the energy production of a core between refueling. Although a fuel assembly would be more expensive to produce, the resulting increase in fuel burnup would most probably result in net fuel costs being cheaper. Increasing burnup extends cycle lifetime and improves the reactor's capacity factor. This in turn results in less radioactive waste per unit energy produced from nuclear reactors by reducing the overall fuel supply. Additionally, HALEU fuels are crucial for the economic viability of multiple gen IV reactor designs. These fuels are also being considered for use in advanced medical isotope reactors and for nuclear thermal propulsion in rockets (Nagley, 2020).

Despite the benefits of HALEU fuels, there are many concerns that must be addressed before they can be used for commercial power production. There is significantly less empirical data for HALEU fuel than there is for low enriched uranium (LEU) fuel. This may affect reactor design because the effects of HALEU level enrichments on material corrosion, core neutronics, and radiation shielding are more difficult to predict than for LEU fuels. Implementing HALEU fuels may also prove challenging due to a current lack of HALEU supply-chain infrastructure. No fuel enrichment facilities have the capability to mass produce HALEU fuels. Although a demonstration of HALEU production using existing enrichment techniques is currently being pursued by the DOE

(Department of Energy), there is no short-term method for producing HALEU fuels other than using down-blending techniques to deplete existing high enriched uranium stores (U.s. doe., 2020; Moe, 2019). This would require new laws and regulations allowing the use of HALEU fuels for commercial power production (Moe, 2019). Furthermore, new laws, regulations, and testing are needed for HALEU packaging and transportation (U.s. doe., 2020). In fact, many experts consider increasing enrichments to HALEU levels to be a considerable nonproliferation risk; feedstock at 20 w/o enrichment requires roughly one-third of the mass to produce weapons grade uranium than feedstock at 5 w/o (Prasad et al., 2015).

Although HALEU fuel is typically considered for use in thermal reactors, they may also be used in fast-breeder reactors (Prasad et al., 2015). Thus, the most standard forms of HALEU fuel would be metallic (pure uranium) and ceramic (UO_2). TRISO fuel, in the form of coated fuel spheres comprised of enriched U_3O_8, is a highly considered alternative form (Collin, 2016). Other forms of HALEU include salts (UF_4), uranium nitrides, and uranium silicides (Wilson et al., 2018).

1.3. Objective of this study

Although many light water based SMRs can operate with fuel enrichments under 5 w/o, HALEU fuels are expected to make these concepts more economically competitive. Allowing SMRs and micro-reactors to utilize HALEU fuels will reduce the overall LCOE. Due to the relatively low capital risk when compared to a large reactor, small reactor designs will be an attractive opportunity to test HALEU fuels for commercial power production. Furthermore, micro-reactors intended for operation in remote towns, such as Oklo's design, could benefit from longer operation times due to the high cost of fuel transport. For these reasons, implementing HALEU fuels in light water based SMR and micro-reactor designs may be the next step in advancing SMR technology. However, there are numerous implications on reactor design and operation that are affected by increasing a reactor's enrichment. These implications apply to the whole spectrum of reactor design including neutronics, thermal-hydraulics safety, materials, and economics considerations.

Motivated by this observation, this study intends to examine each of these implications in more detail and embark on a case study of a small modular LWR type reactor as a concrete demonstration of these implications. The NuScale's 160 MWt SMR concept (U.S. NRC., 2012) was chosen as the example reactor in the case study. The NuScale SMR was selected in the case study for the following reasons: (1) It is far along in the NRC licensing process and can realistically start producing commercial power within 10 years (A demonstration reactor is projected to be completed by 2024) (Wna, 2020). (2) It is based off standard PWR designs, of which, the economics and engineering design parameters have been thoroughly studied. Moreover, the results of this study can easily be related to other LWR designs. (3) It uses uranium oxide fuel, which has well-known mechanical and neutronic properties and fabrication costs, while other novel fuel forms such as TRISO fuels contain more uncertainty. It should be noted that although the case study was conducted on the effects of increasing fuel enrichment on NuScale's SMR design, the overall effects of HALEU fuels on SMRs and micro-reactors can be generally understood.

The rest of the paper is organized as follows: Section 2 provides a generic yet in-depth discussion on the HALEU fuel implications in the aspect of neutronics, thermal-hydraulics safety, materials, and economics considerations towards the reactor design. Section 3 presents the results of a case study employing a small modular LWR type reactor with HALEU fuels. The emphasis of the case study was paid to the performance differences of the reactor with non-HALEU fuels. The reactor design methodology and optimization procedure are also introduced in this section. The last section (Section 4) offers some concluding remarks of this study.

2. HALEU fuel implications

As mentioned earlier, increasing the enrichment of uranium fuel can change the operation of a nuclear reactor in many ways. Any of these changes may either directly or indirectly act as a limiting factor for the operability of a reactor. This section outlines the most significant effects of HALEU fuel implementation in SMRs and purposely categorizes these effects into five different aspects: neutronics, thermal-hydraulics, safety, materials, and economics. The aim of the discussion is to provide a theoretical guidance to interpret the results of the case study discussed in Section 3, and for those effects not examined in the case study, to provide a general overview of expected results to be tested in the future.

2.1. Neutronics considerations

2.1.1. Global peaking factor

The most prominent physical effect that comes as a response to higher enriched fuel is higher power peaking factors, the ratio of the maximum to average core power density. The maximum achievable power density is dependent on certain critical conditions within the core such as the peak centerline fuel temperature, peak cladding temperature, and fuel rod internal pressure (Lewis, 2008). For the case of a typical PWR, the cladding temperature is the limiting factor for the maximum global peaking factor (GPF), the maximum power-peaking factor at a single point of time in the reactor core. The maximum allowable GPF is unique for each core design (Wu, 2016; Wu et al., 2017) but is set to ensure that cladding temperature does not exceed 2200 °F (U.s. nrc., 2012). By increasing fuel enrichment, there will be a greater difference in enrichment at any given cycle time between fresh, once-burned, and twice-burned fuel assemblies, resulting in a greater variance in power distribution and fuel temperatures. This effect can be controlled by changing the positioning of control rods and the concentration of burnable poisons. Most neutronics and thermodynamics repercussions of increasing enrichment come as a response of this effect. Perhaps most evident, is the corresponding increase in peak fuel temperature, which leads to lower local coolant density and a reduction in neutron backscatter, or the portion of neutrons that are reflected towards the fuel rods. Likewise, an increase in fuel temperature causes Doppler broadening of the resonance capture cross sections in uranium, which effectively reduces neutron resonance escape probability. These effects are known as moderator and fuel temperature reactivity feedback.

2.1.2. Reactivity coefficients

Moderator and fuel temperature reactivity feedback coefficients, α_m and α_f, which determine the effectiveness of reactivity feedback in a reactor core, are determined mainly by core design and fuel enrichment. More negative reactivity feedback coefficients represent quicker and more stable responses to changes in reactivity (Wna, 2020). Positive reactivity feedback coefficients represent unstable responses to changes in reactivity. One of the dangers involved in increasing the fuel enrichment in a commercial nuclear reactor core is that both moderator and fuel temperature reactivity feedback coefficients increase in value, that is they become less negative (Hirai, 1990). The fuel temperature coefficient becomes less effective at higher enrichments because of an increase in the fission rate while at the same time, the radiative capture rate decreases (Hirai, 1990). Likewise, the moderator feedback coefficient becomes less negative because of increased boron and lithium hydroxide solution in water which collectively contribute to a higher net neutron absorption rate (Hirai, 1990). Due to these effects, as enrichment increases there is an overall reduction in the negative reactivity feedback effect from changes in temperature within the core.

2.1.3. Burnable poison concentration

As mentioned above, higher enriched fuel is expected to require a higher level of burnable poison to maintain constant power levels. This problem cannot solely be solved by increasing the levels of boric acid in the coolant as this may change the density response of the moderator and reduce the moderator feedback to unsafe levels (Hirai, 1990). In extreme cases, an over-borated moderator can lead to an over-moderated state where there is an overall decrease in the absorption of neutrons with higher power, resulting in an increased fission rate. To combat this issue, lumped burnable poison (LBP) in the form of Gd_2O_3 is used in place of additional boric acid to hold down the excess core reactivity and maintain criticality. The LBP is typically inserted into the core inside of selected fuel rods. Higher LBP content is needed in a PWR core in order to attain longer fuel cycles and maintain optimal power distribution. Increasing the relative density of the LBP in the fueling turn is likely to increase in the possibility of cracks forming within the fuel in the fabrication process due to a noticeable difference in thermal expansion coefficients between Gd_2O_3 and UO_2 (Hirai, 1990). Additionally, higher LBP content results in a more positive fuel temperature coefficient, although this effect is less significant than the effect on the moderator temperature feedback coefficient from high boron content (Burns et al., 2020). Moreover, increased LBP concentration may result in an overall decrease in the thermal conductivity of fuel due to Gd_2O_3 having a lower thermal conductivity than UO_2 (Burns et al., 2020). BWRs do not suffer from this problem as they control reactivity by actively changing control rod position, core pressure, and coolant mass flow rate.

2.1.4. Flux and fission product concentration

With adjustments from reactivity control systems as mentioned above, the core-averaged neutron flux should not change considerably with increased enrichment; however, the resulting perturbation to power distribution leads to higher local flux peaks around fresh fuel batches. This suggests higher rates of material irradiation exposure and zirconium alloy corrosion from higher local temperatures. Additionally, higher fluxes result in increased equilibrium concentrations of fission products like ^{135}Xe, which has a significantly high thermal neutron absorption cross-section (Lewis, 2008). Alternatively, the concentrations of stable fission product poisons, like ^{149}Sm, are less affected by changes in flux, although there is still expected to be some change (Lewis, 2008).

In addition to changes in flux distribution, the utilization of HALEU fuel may also result in an overall reduction in thermal neutron flux. Thermal flux decreases at higher enrichments for all stages of a reactor fuel cycle (Burns et al., 2020). Higher enriched uranium fuel has a higher fission neutron yield at higher neutron energies. At the end-of-life (EOL) of a fuel cycle, the flux differences between enrichments become less significant due to the buildup of fission product poisons, which increases overall neutron absorption.

2.1.5. Fuel cycle

The implementation of HALEU fuel has several important impacts on the entire fuel cycle. At the front-end of fuel cycle, a significant increase in the natural uranium feedstock is necessary to produce a fresh batch of HALEU fuel. This increase in natural uranium feedstock is offset somewhat by a decrease in the required fuel supply due to a reduction in refueling frequency. This results in an overall increase in disposed depleted uranium (DU) with increased enrichment (Burns et al., 2020). The low-level radioactive waste (LLW), defined as items contaminated with radioactive material, is also expected to increase due to the added separative work necessary to enrich product fuel (Burns et al., 2020; U.S. NRC., 2017). During the operation of a HALEU fuel core, there is expected to be an overall decrease in high-level radioactive waste (HLW) in the form of spent nuclear fuel (SNF) due to the prolonged fuel lifetime. Consequently, this HLW decrease in SNF allows for a net decrease in land use and carbon emission per unit of energy produced (Burns et al., 2020). However, due to the increased work needed in the front-end fuel cycle, water usage increases slightly with enrichment (Burns et al., 2020). At the back-end of the fuel cycle, the higher burnup of HALEU fuel results in changes in SNF characteristics such as changes in decay heat and radioactivity over time (Burns et al., 2020). In the very short and very long time frames, the decay heat of higher enriched spent fuel was calculated to be lower than that of less enriched fuel mainly due to a reduction in fissile material in higher burnup fuel. In the intermediate time frame (~4–100 years), the decay heat of higher enriched spent fuel was found to be slightly greater than that of lower enriched fuel due to more fission product buildup. The net activity of spent fuel after 100 years of decay time is expected to slightly decrease with increasing enrichment due to a reduction in actinide concentration which is mostly balanced-out by an increase in radioactive fission-products (Burns et al., 2020).

It is worth mentioning that the decrease in actinides can be beneficial from a nonproliferation standpoint because the ^{239}Pu and ^{241}Pu contents are reduced in higher burnup SNF (U.S. NRC., 2017). By reducing the concentration of ^{238}U in fresh fuel, the concentration of ^{239}Pu is expected to be reduced in spent fuel. Additionally, the higher burnup in a HALEU reactor would result in a higher utilization of fissile ^{239}Pu and ^{241}Pu contents (Beller and Krakowski, 1999). Therefore, the SNF of a PWR is proposed to be more proliferation resistant by increasing fuel burnup.

2.2. Thermal-Hydraulics considerations

Changes in some parameters like the rate of control rod adjustments and burnable poison concentration allow for a reactor to maintain a consistent power level with higher enriched fuel. Consequently, the average volumetric power density and coolant temperature essentially remains the same. This suggests that implementing HALEU fuel in SMRs would have no significant impact on the plant thermal-hydraulics performance, but it may require additional LBP fuel rods to compensate for increased enrichments and result in different axial profiles. The most significant effects would likely come as a result of increased boron concentration. As a side-effect, increasing boron concentration in a core will increase the radioactivity in the primary heat transfer loop. This is because higher boron concentrations raise the rate of (n, ^{10}B) reactions, which produce radioactive tritium isotopes in the coolant (Burns et al., 2020). Moreover, higher boron concentrations increase the occurrence of crystalized boron deposits within the primary loop and accelerate crud depositing that may result in an axial offset anomaly (AOA) (Li et al., 2019).

2.3. Safety considerations

Many of the above thermal-hydraulics related design implications involved with increasing the enrichment of nuclear fuels to HALEU levels may compromise a reactor design by exceeding NRC regulations and general safety limits. Although SMRs and micro-reactors have embraced many passive safety design features, higher enriched fuel, higher fuel burnup, longer cycle time, and higher boron concentration still would increase the likelihood of accidents during reactor operation. Boron content may affect reactor safety by increasing the overall likelihood of reactivity excursion events from dislodged boron crud being carried through the core (D'Auria, 2017). During such an event, negative reactivity is introduced causing a local drop in moderator temperature. On the other hand, positive reactivity from reflux condensation events might become more severe in higher enriched cores. These events occur when a small break causes the buildup of boron-diluted water in the steam generator tubes which can re-enter into a heavily borated core during operation (Li et al., 2019). As a result, the local boron concentration in the region near the coolant inlet of the core will reduce by a significant margin. This reduction in boron concentration leads to an increase in local reactivity, which may be a serious safety risk. While reflux condensation occurs at the same frequency regardless of enrichment, the higher boron concentration in a higher enriched core results in an increased sensitivity to these events.

Additionally, by extending fuel cycle life with further enriched fuel, certain safety concerns must be addressed during the core design. One major concern is the GPF limit. To maintain a peak cladding temperature of under 2200 ℉, assembly positioning and LBP concentration in fuel must be optimized to allow for a small power differential across the core. Higher enriched fuel and an increase in crud deposition naturally can lead to greater axial power offset. Since plants have limits on the level of axial offset between the upper and lower regions of the core, this effect may result in premature shutdown (Odette and Zinkle, 2019). Another major safety concern is the soluble boron limit of a reactor. High boron levels would contribute to crud deposition, limit the response of moderator feedback, increase the radioactive quality of coolant in the primary loop (a concern in the case of a small break accident) (U.S. NRC., 2018), and may result in a reactivity-initiated accident in the case of heterogeneities in boron concentration or the dislodging of solid borated matter. While some of these effects constitute the limiting parameters of design regarding boron concentration, it is a common practice for PWR type reactors to keep initial boron concentration below 2000 ppm (D'Auria, 2017). Keep in mind that the true limiting factor for the boron concentration is to maintain a moderator temperature coefficient at or below zero, and the boron concentration should be limited accordingly.

The materials within a reactor must also withstand the expected increase in corrosion and radiation that causes embrittlement and degradation. Particularly, the increased radiation exposure, crud deposition, and radioactive content in coolant may compromise the integrity of the reactor components, especially by increasing the likelihood of cladding failure. Changes in cladding creep, fuel pin swelling, fission gas release, and crack formation must be considered. Oxide layer formation, fission gas release, and the formation of high burnup structures (HBS) (A surface structure unique to uranium oxide fuel at high burnup) are all expected to affect the heat transfer characteristics of fuel rods.

Regarding the concerns on the transport of nuclear materials, HALEU fuel requires considerably less work compared to the weapons grade uranium, which presents a great risk during transport. The numerous supply lines needed for SMRs and microreactors compared to large reactors adds more concern, especially with microreactors serving remote communities as the long supply lines introduce added risk. Additional transportation safety concerns such as higher radioactivity and greater concerns on criticality risk increase transportation standards for HALEU fuel and UF_6 (Eidelpes, 2019). On the other hand, the increased burnup of HALEU fuel allows for more proliferation resistant spent fuel. Moreover, the longer cycle time from HALEU utilization allows for less radioactive waste with lower actinide concentration.

For the reasons mentioned above, an SMR or micro-reactor plant design must be reevaluated to ensure that the utilization of HALEU fuel does not result in a violation of their respective thermal–hydraulic safety constraints. The safety constraints and technical specifications vary between reactor designs with some operating limits varying between individual reactors, and since there are no SMRs or micro-reactors currently operating in the United States, the NRC has not published any official technical specification documents on these subjects (U.S. NRC., 2019). Key safety constraints of a typical PWR design are summarized in Table 2. The values shown in Table 2 are either directly mentioned by the NRC as a technical specification or are included in the core operating limits report (COLR) of a reactor of that design (U.S. NRC., 2012; U.S. NRC., 2020; U.S. NRC., 2020; R.E. Ginna Nuclear Power Plant., 2018; U.S. NRC., 2007; U.S. NRC., 2010; U.S. NRC., 2011). While these safety constraints do not directly apply to SMRs or micro-reactors, they may work as a "sanity check" to ensure that PWR type reactors can operate safely using HALEU fuel.

Table 2
Safety Constraints of Current or New PWR Designs.

Limit	Max/Min	Reactor Type	
Fuel Centerline Temp.	<	5080–0.0058*B ℉ [1]	5080–0.0065*B ℉ [1]
RCS Pressure	<=	2735 psig	2750 psig
RCS Flow	>=	284,000 gpm	139.7E6 lb/hr
RCS Avg. Coolant Temp.	<=	580 ℉ [2]	604.6F
Coolant Spec. Act.	<=	100 mCi/gm	100 mCi/gm
Cladding Temp.	<=	2200F	2200F
MTC	<=	0 pcm/℉ [2]	
GPF	<=	2.6 [2]	2.5 [3]
Axial Flux Difference	<=,>=	6, −12% [2]	17.51, −16.26 % [4]
Boron Conc.	<=	2000 ppm [5]	2504 ppm [6]

[1] 'B' represents core averaged burnup in MWD/MTU
[2] COLR for R. E. Ginna Nuclear Power Plant (R.E. Ginna Nuclear Power Plant., 2018)
[3] COLR for Arkansas Nuclear One – Unit 1 (U.S. NRC., 2007)
[4] Example from B&W Crosstraining Course Manual (U.S. NRC., 2010)
[5] COLR for Prarie Island Nuclear Generating Plant Unit 1 (U.S. NRC., 2011)
[6] Operating Maximum, Not Technical Specification

2.4. Material considerations

Increased neutron fluence is the first concern for material considerations for a HALEU core. Increasing radiation exposure of fuel and cladding material is one of the most significant consequences of increasing core burnup. Although the neutron flux throughout a PWR core does not change much as a response to higher enriched fuel (Burns et al., 2020), the exposure time is increased significantly. This requires fuel and cladding material to be able to withstand higher levels of neutron fluence, or neutron dose per unit area. Also affected is the reactor pressure vessel (RPV) of the core. Since HALEU cores can achieve longer cycle times with negligible increases in shutdown time, the RPV may be exposed to a higher lifetime neutron fluence. This increase in fluence within the reactor may cause higher levels of irradiation embrittlement and the loss of fracture toughness due to radiation induced corrosion. Neutron irradiation has the tendency to increase the ductile-to-brittle transition temperature, which increases the risk of brittle failure in ferritic RPVs (Nrc, 2019). Irradiation induced corrosion is also dependent on core temperature. Neutrons above 0.5 MeV are most effective at displacing atoms in a ferritic material at operating temperatures between 260 and 300 °C (Nrc, 2019). Although RPVs do not have a precise neutron fluence limit, an RPV that is exposed to more than $10^{17} n/cm^2$ with $E > 1$ MeV is required by the NRC to perform material surveillance (Burns et al., 2020). This material surveillance program involves conducting fracture toughness tests on material samples withdrawn from a reactor vessel. Changes in material properties due to radiation exposure and high temperatures and pressures are tested against ASME standards that determine the operability of a reactor (Nrc, 2019; Nrc, 2019).

Another concern is the mechanical properties of reactor components as they change with temperature. The average core fuel and moderator temperatures are expected to remain the same with increased fuel enrichment to allow for consistent thermal power output. However, higher fresh fuel enrichment suggests larger enrichment differences between batches, which implies greater temperature gradients within the core, and thus higher peak fuel and cladding temperatures. Increased peak cladding temperatures are the limiting factor of core temperature because zirconium has a much lower melting temperature than UO_2. Furthermore, zirconium alloy is susceptible to thermal creep at high temperatures (Adamson et al., 2019). Because of this, small differences in cladding thickness along the vertical axis may result in a higher likelihood of failure. Additionally, increases in local temperature will lead to an increase in local fuel swelling.

A much more problematic issue in this regard is the increased corrosive effects due to prolonged zirconium-water interaction in PWRs and BWRs. Waterside corrosion may significantly reduce the structural integrity of zirconium cladding. This phenomenon occurs due to multiple compounding reasons but is primarily due to cladding thinning, where the outside surface is chemically altered to form a brittle oxide layer. There is a design limit that states this oxide layer must be no thicker than ~ 100 μm (Odette and Zinkle, 2019). Also worth noting are the effects of hydride embrittlement. Hydride embrittlement occurs when hydrogen is introduced interstitially within the cladding material. This hydrogen can be introduced at the cladding-water interface where Zr-H_2O reactions produce hydrogen as a byproduct. These hydrogen atoms bond with lithium to form hydrides. These hydrides ultimately embrittle the zirconium alloy (Chan, 1996).

Oxide layer formation is accelerated by crud deposition. The term 'crud' refers to irradiated, eroded, and corroded non-fuel materials that are deposited on cladding surfaces. Crud deposition can be aided by low pH levels from the use of soluble boric acid as a burnable neutron poison, which is balanced by dissolving lithium hydroxide in the primary loop. Furthermore, crud deposits in PWRs form evenly distributed layers outside the oxide layer of cladding. By impeding heat transfer, crud deposits can cause local boiling and exacerbate corrosion and crud buildup, establishing a positive feedback loop (Odette and Zinkle, 2019). Due to these reasons, crud buildup is the primary concern when it comes to corrosion-related fuel rod failure. Of the four corrosion accidents since 1990, all of them were due to crud-induced corrosion (Odette and Zinkle, 2019). Moreover, crud buildup may affect plant thermal-hydraulics by causing an axial offset anomaly which may lead to a premature shutdown. By prolonging a reactor's fuel cycle, its cladding material will be exposed to higher levels of corrosion and crud deposition. Because of this, SMR designs that use HALEU fuel must pay careful attention to primary loop chemistry.

The production of fission gasses is a major factor that affects the fuel heat transfer capability. With increased burnup from the utilization of HALEU fuels, it is expected that enhanced fission gas release will result in a reduction in thermal conductivity and an increase in inner-tube pressure. Approximately 15% of all fission products are the noble gases xenon and krypton which have low solubility in UO_2 (Rest et al., 2019). These fission gasses will form bubbles within and in-between grain boundaries, and after being exposed to significant levels of burnup, will diffuse outside the fuel pellet boundary and inhabit the fuel-cladding gap. These fission gasses have significantly lower thermal conductivities than helium resulting in a more insulated fuel-gap region. This phenomenon causes fuel temperatures to become higher, although the overall effect remains that fuel temperatures decrease with burnup. The level of fission gas release for a fuel rod depends on fuel defect concentration, grain size, availability of migration pathways, temperature, and burnup. Additionally, high burnup fuel tends to release high levels of fission gas when exposed to sharp changes in temperature (Une et al., 2006). Due to this reason, twice-burned fuel batches in a HALEU core may suffer most from fission gas release immediately after startup. Moreover, fission gas release increases exponentially with burnup regardless of temperature (Rest et al., 2019). Fission gas buildup can create high pressure inter-granular bubbles that induce cracks that reduce the mechanical integrity, heat transfer, and neutronics properties of fuel. The effect of fission gas release on thermal diffusivity is inversely dependent on local burnup up to roughly 70 MWd/kgU, at which point the steepness of the slope is reduced due to the development of a complex microstructure known as high burnup structure (HBS) on the rim region of the fuel (Rest et al., 2019). Due to high neutron absorption at pellet surfaces, there is a higher plutonium content which causes high local burnup and grain recrystallization, creating quasi-spherical micropores. While HBS reduces the thermal conductivity of the uranium fuel itself, its overall effect on thermal conductivity is beneficial because HBS pores act as fission gas sinks, reducing the overall effects of fission gas release (Rest et al., 2019).

The last material consideration worth mentioning is that changes in reactor burnup have a significant effect on the rod internal pressure (RIP) of fuel rods. RIP does not significantly contribute to fuel failure during normal operation (Odette and Zinkle, 2019) other than the increased hydride reorientation that is known to embrittle cladding (Chan, 1996). However, RIP is a serious concern regarding spent fuel storage (Machiels et al., 2017; Kim et al., 2017). It has been reported that the major variables that may cause cladding failure in dry cask storage are the hoop stress caused by rod internal pressure and cladding temperature that arises from decay heat (Kim et al., 2013). This is worsened by cladding material degradation from oxide layer formation, hydrogen concentration, and irradiation embrittlement. Further material degradation is reduced during storage due to NRC guidelines that restrict allowable cladding temperature to 400 °C (Kim et al., 2017). Since fission gas is released at an accelerated rate with increasing burnup, the risk of cladding rupture from hoop-stress becomes greater (Kim et al., 2017). Case studies on large reactors showed a wide range of hoop stresses recorded at 400 °C up to 55 GWd/MTU; at this burnup level, discharge hoop stress of up to 120 MPa was recorded; the NRC limits spent fuel cladding to 90 MPa for high burnup fuel (Kim et al., 2013). Due to concerns regarding dry storage and reductions in thermal conductivity, expanding the fuel cycle length of SMRs and micro-reactors requires additional research. On the other hand, there is an overall decrease in discharged spent fuel decay heat, HLW content, and land use requirements at higher enrichments (Burns et al., 2020). One possible option for reducing the positive feedback "poisoning" effects from fission gasses involves a higher initial pressure for the helium backfill gas. This allows for better axial transport of fission gas by restricting closed gaps from forming due to fuel-clad interaction (Turnbull, et al., 2020).

The reduction in structural integrity of cladding material that comes from the accumulation of embrittlement and stress effects mentioned in this section may not only limit the total life of cladding material in a reactor but may also increase the risk of cladding bursting that may result from a loss of coolant accident (LOCA) (Gussev et al., 2015).

2.5. *Economic considerations*

Because the implementation of HALEU fuels is mainly considered for their potential economic benefits, their ability to improve the economic efficiency of a nuclear power plant must be justified. The main method for reducing plant costs include increasing revenue by improving the capacity factor by increasing operation length and lowering fuel costs by reducing the overall mass of the required fuel. HALEU fuel may potentially prolong a nuclear reactor's fuel cycle by increasing the maximum achievable fuel burnup without significantly impacting overall capital costs and operation and maintenance (O&M) costs. By increasing the duration of power production, a higher enriched reactor may reduce its refueling frequency, thus allowing for improved reactor economy depending on how much extra cost is associated with increasing fuel enrichment. Although the cost per kilogram of HALEU fuel is expected to increase, it is still expected that the overall cost of fuel will decrease due to a reduced frequency of refueling. The extra cost of HALEU fuel may mostly be attributed to the increase in feed uranium needed to produce the same mass as LEU; however, there are other contributing costs that must be considered. First, due to higher radiation and proliferation risks, more demanding standards for transportation and packaging regulations might be introduced, which may increase the cost of fuel transportation. Early batches of HALEU fuel may be cost-prohibitive because there is currently no existing supply chain for fuels above 5 w/o enrichment. Moreover, since higher burnup is to extend reactor cycle length required, higher fuel fabrication costs may be necessary since the fuel must be designed to reduce the effects of additional mechanical stress, corrosion, and radiation embrittlement (Pimentel, 2019). Since fuel suppliers are currently developing and have already developed advanced accident tolerant fuels which are better suited for high burnup environments (Pimentel, 2019), the level of investment needed for HALEU fuel to become readily available for commercial power producers is mainly tied to technologies which allow for large-scale manufacturing and transportation of accident tolerant fuels rather than for the development of the technology itself. Lastly, due to an expected increase in neutron fluence over the reactor lifetime from longer operation cycles, the reactor pressure vessel (RPV) may experience a reduction in operational lifetime.

Ref. (Carlson et al., 2020) provides more detailed information on the economic effects of increasing fuel enrichment and the method for determining resulting cost reductions. It is important to note that the LCOE (levelized cost of energy) of a power plant is defined as the cost of generating a single unit of energy and is used to estimate a return on the capital invested, often expressed in units of \$/MWh. This parameter may be calculated using Eq. (1) below,

$$LCOE = \frac{C_{cc} + C_{O\&M} + C_U}{P \cdot \eta \cdot T_{cycle}} \tag{1}$$

where C_{cc}, $C_{O\&M}$, and C_U represent the cycle averaged capital, O&M, and fuel costs respectively while η is power plant capacity factor, P is the rated unit power, and T_{cycle} is the total fuel cycle length. It must be noted that to increase its LCOE, a reactor cannot simply extend cycle time by reducing power output. Although there are benefits with increasing cycle time as shown in Eq. (1), these benefits are effectively cancelled out due to a reduction in power. For this study, the tested designs are assumed to operate at full-power while operational and zero-power when offline for refueling; hence, the capacity factor and cycle time are only impacted by the differences in fuel burnup due to changes in fuel enrichment.

3. Case study

A case study with the NuScale's 160 MWt SMR as the example reactor was carried out in this section. The purpose of the case study was to provide analytical evidence in support of the implications of the use of HALEU fuel in SMRs and micro-reactors identified in section 2. This was accomplished by using a computational reactor model of HALEU fueled NuScale SMR to evaluate its impact on core neutronics including the changes in fuel cycle and spent fuel composition, thermal hydraulics, and plant economics. The Studsvik Scandpower reactor physics codes (Gussev et al., 2015) were used to model a standard NuScale's 160 MWt SMR design and a customized version optimized for a 48-month fuel cycle operation. Through the comparison of the simulation results, changes in key parameters were quantified to understand the impact of HALEU on the SMR. The fuel management scheme used in the SMR design was that of a 48-month and three-batch fuel cycle employing NuScale's fuel assembly design. For reactor security and safety considerations, only analysis results that met current NRC licensing standards such as those provided in Table 2 and NuScale's key safety standards (Welter, 2010), including a GPF of under 2 and a reactor coolant system (RCS) boron concentration of under 2,000 ppm, were deemed acceptable for the study. In the rest of this section, a brief introduction of the computational modeling approach is provided first, followed with calculation results and discussions. Although some results require additional analytical methods, most of the analysis results discussed in this section are direct outputs from SIMULATE, which is the core physics simulation code in the Studsvik Scandpower reactor physics code suite (Studsvik, , 2009). If the methods for calculating certain results are not explicitly mentioned, it may be assumed that they are direct outputs from the simulation.

3.1. Methodology

3.1.1. Analysis code description

The neutronics analysis was performed using the Studsvik Scandpower reactor physics code suite (Studsvik, , 2009) which consists CASMO, CMSLink, and SIMULATE codes. CASMO is a two-dimensional, lattice neutron transport code that models the LWR fuel assembly designs. Working in conjunction with the CMSLink code, CASMO uses the data from a cross section library to produce a set of collapsed two-group cross sections as a function of key reactor conditions such as fuel burnup, burnable poison depletion, fuel and coolant temperatures, power, etc. This calculation is performed on a per fuel pin basis with the final output being on a per fuel assembly basis. The resulting two-group cross section library is then used by SIMULATE, which is a three-dimensional, steady-state, nodal code that is used to model and analyze LWR cores. SIMULATE can perform neutronic and thermal–hydraulic coupled calculations on a whole core level, as well as predict core reactivity, power distribution, fuel temperature, and composition. Fig. 1 briefly shows the interaction and data flow of the three codes described above, where ENDF (Evaluated Nuclear Data File) is the microscopic cross-section library.

The thermal–hydraulic and economic analyses were performed using traditional analytic approaches based on the neutronics analysis results. Material implications were unable to be quantified due to a lack of access to the appropriate corresponding simulation software. However, thermal–hydraulic and material concerns are key areas of interest for further study into the effects of increasing enrichment to HALEU levels in SMRs and micro-reactors.

3.1.2. Core optimization and baseline design

A multi-step and iterative optimization process was carried out to obtain an optimal enrichment for a 48-month cycle with the NuScale's core design. First, the enrichment values of the three fresh fuel batches were adjusted so that the average fresh batch enrichment was within the HALEU range of enrichments. Next, the individual assembly was optimized to reduce the pin (power) peaking factor (PPPF). Fuel assemblies with homogeneous fuel pin enrichments tend to have a higher PPPF than those with varying fuel pin enrichments. To minimize pin peaking factors, individual fuel pin enrichments were adjusted while maintaining the same overall average assembly fuel enrichment. This process is partly illustrated in Fig. 2, which provides the difference in maximum PPPF between a homogeneously enriched fuel assembly and an optimized fuel assembly (only 1/8 assembly is shown due to symmetry). Fig. 2 also shows the calculated infinite multiplication factor (k-inf) for the beginning of cycle (BOC), middle of cycle (MOC), and end of cycle (EOC) of the assembly.

The 48-month optimized equilibrium core is shown in Fig. 3. The center assembly (C-03) of the core is replaced every cycle, while the 12 remaining fresh assemblies (C-01, C-02) are reshuffled during the first refueling to the once-burned (B-01, B-02) fuel assembly locations, and then, following the second refueling, to the twice-burned (A-01, A-02) fuel assembly locations. The maximum attainable core-averaged burnup and cycle time for an equilibrium cycle were predicted by SIMULATE. Fresh fuel enrichments were iteratively adjusted to optimize the maximum cycle burnup to match that of a 48-month cycle core. The final core-layout and assembly enrichments are also shown in Fig. 3. Using an equilibrium fresh-batch loading of six assemblies at 9.10 w/o, six assemblies at 8.1 w/o, and one center-core assembly at 5.2 w/o, the average equilibrium fresh fuel enrichment is found to be 8.34 w/o. It should be noted, however, that nonhomogeneous fuel pin enrichments may result in increased manufacturing costs due to the need to segregate fuel pins of different enrichments during the manufacturing process.

3.2. Neutronics analysis results

3.2.1. Power and flux profile

As mentioned in Section 2.2.1, the GPF of a reactor core is one of the most important reactor safety metrics and needs to be minimized during the core design phase. GPF values can be produced by SIMULATE as a function of burnup. Fig. 4 displays the GPF curve of NuScale's standard 24-month cycle and the customized 48-month cycle. The maximum burnup for the 24-month core and 48-month core are 12.5 and 24.2 GWd/MT, respectively. As shown in Fig. 4, the GPF is higher at all stages during the operation of a HALEU core. This is likely due to larger differences in fuel assembly enrichment as shown in Fig. 4. This effect is to a great extent minimized by the increase in burnable poison in the

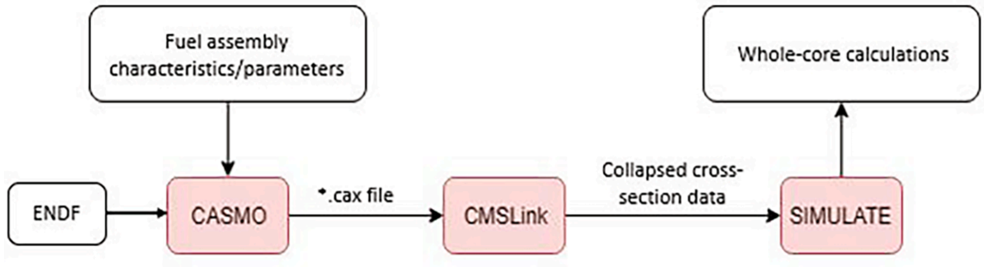

Fig. 1. CASMO, CMSLink, and SIMULATE computational steps.

Unoptimized 1/8 Assembly Pin Enrichments

0.00%								
5.80%	5.80%							
5.80%	5.80%	5.80%						
0.00%	5.80%	5.80%	0.00%					
5.80%	5.80%	5.80%	5.80%	5.80%				
5.80%	5.80%	5.80%	5.80%	5.80%	0.00%			
0.00%	5.80%	5.80%	0.00%	5.80%	5.80%	5.80%		
5.80%	5.80%	5.80%	5.80%	5.80%	5.80%	5.80%	5.80%	
5.80%	5.80%	5.80%	5.80%	5.80%	5.80%	5.80%	5.80%	5.80%

Optimized 1/8 Assembly Pin Enrichments

0.00%								
6.49%	6.04%							
6.04%	6.49%	6.04%						
0.00%	6.04%	5.74%	0.00%					
6.04%	6.04%	6.04%	6.04%	6.04%				
6.04%	6.04%	6.04%	5.74%	5.74%	0.00%			
0.00%	6.04%	6.04%	0.00%	5.44%	5.74%	6.04%		
5.44%	5.74%	6.04%	5.44%	5.44%	5.74%	6.04%	5.74%	
5.44%	5.44%	5.44%	5.44%	5.44%	5.44%	5.44%	5.44%	5.13%

Indicates CR guide tube/instrument tube
Indicates Gd2O3 fuel pin
Indicates normal fuel pin

Unoptimized		Optimized	
Average assembly enrichment:	5.800%	**Average assembly enrichment:**	5.800%
Max BOC pin peaking factor:	1.1330	**Max BOC pin peaking factor:**	1.0850
Max EOC pin peaking factor:	1.0570	**Max EOC pin peaking factor:**	1.0640
BOC k-inf (0 MWd/kg):	1.19522	**BOC k-inf (0 MWd/kg):**	1.19565
MOC k-inf (12.5 MWd/kg):	1.16012	**MOC k-inf (12.5 MWd/kg):**	1.15961
EOC k-inf (25 MWd/kg):	1.16948	**EOC k-inf (25 MWd/kg):**	1.16728

Fig. 2. Optimized 5.8 w/o fuel assembly with burnable poisons.

HALEU core. It is also important to note that the difference between maximum GPF is very small. The maximum GPF of the 24-month and 48-month cycles are 1.82 and 1.86, respectively. Considering the maximum allowable GPF is 2.0 as given in the NuScale's design specification (Welter, 2010), the HALEU core is proven to be able to operate normally with little consequence from a power profile perspective.

The 48-month cycle core design also experiences an increase in axial offset. Fig. 5 shows this trend. Increased fuel enrichment is shown to have marginal effect on the axial offset of a PWR type core at BOC; the higher enriched core shows a slightly greater average axial offset on the range of 0–12 GWd/MTU. However, the effect of increased core burnup has a greater effect on EOC axial offset with a final value of −2.4%. Although this effect is not preferable, it shows that both cores fall well within standard allowable ranges as shown in Table 2. However, the trend shown by the 48-month cycle suggests that further increasing core burnup may result in unsafe axial offset values. Depending on the safety constraints of a reactor, this factor may set a limit on the maximum enrichment to be utilized in a PWR type SMR.

The core average flux behavior for higher enriched core has shown some phenomenal differences when compared to that of standardly enriched cores. Fig. 6 shows the average flux level along with the average burnup for both the 24-month and 48-month cycle cores. As can be seen, the higher enriched core has an overall reduction in the flux level compared to the low enriched core. The average total flux reduction up to the burnup 12 GWd/MTU is ~ 7%. Furthermore, the fast to thermal flux ratio in the higher enriched core increased from 7.87% to 12.87%, which indicates the fission contribution from fast neutrons increased in higher enriched core. This effect is likely due to an overall increase in neutron capture rather than leakage, which is considerably lower for higher enriched cores as shown in Fig. 7. For a fission reactor core to maintain the same power with higher enriched fuel, flux must be reduced. This is because, as the number of fissile isotopes increases, so does the macroscopic fission cross section. To maintain a constant core-averaged rate of thermal power, the flux must be controlled by increasing neutron capture or leakage. This would also explain why there is a more significant difference in thermal flux between the two cores. Some factors that contribute to a higher rate of neutron capture in higher enriched cores include lower resonance escape probabilities from a higher concentration of ^{235}U, an overall increase in boron concentration, and an increase in fission bred poisons. This decrease in flux may positively affect safety concerns due to a decrease in the neutron fluence exposure of the RPV and reactor components.

3.2.2. Boron concentration

As mentioned in **Section 2.2.3**, to achieve higher burnup with higher fuel enrichments, more burnable poison must be used to maintain criticality at the same power level. Because of this, the 48-month cycle reactor uses substantially more boric acid compared to the 24-month cycle as shown in Fig. 8. The maximum boron concentration in the 48-month reactor is 1757 ppm, while that of the 24-month reactor is

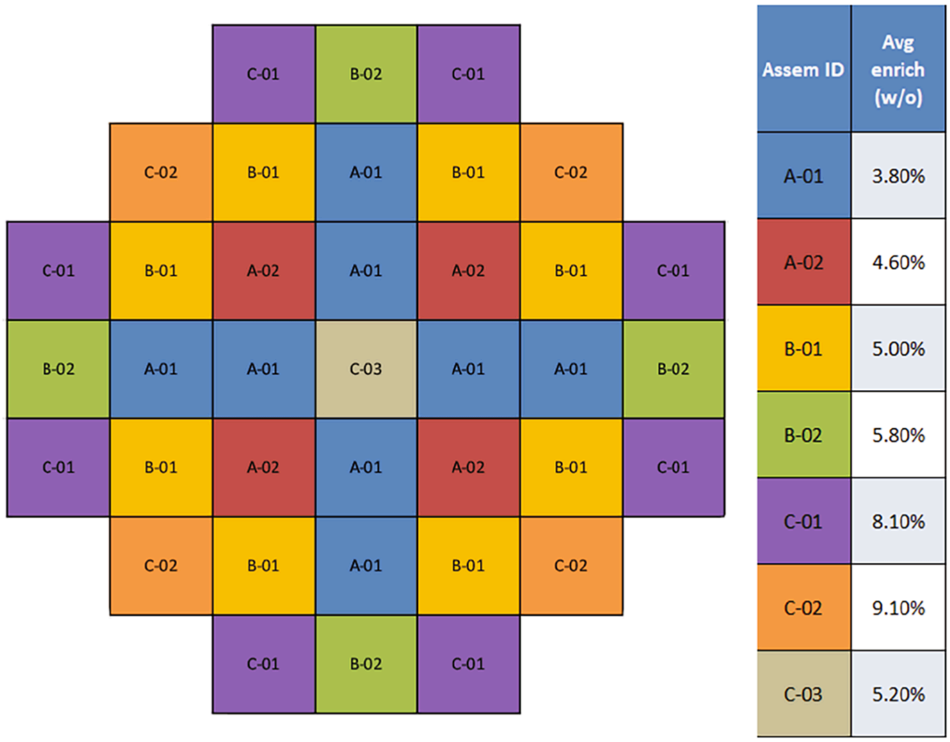

Fig. 3. The baseline 48-month out-in fuel management scheme loading pattern map.

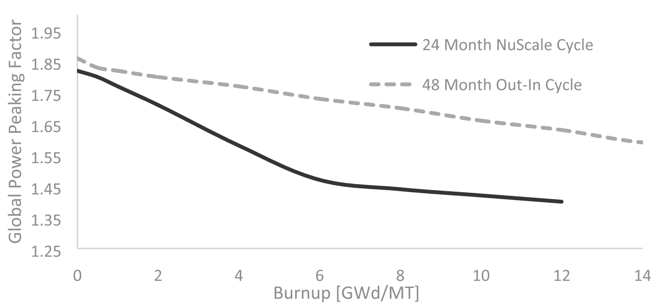

Fig. 4. Global peaking factor curve.

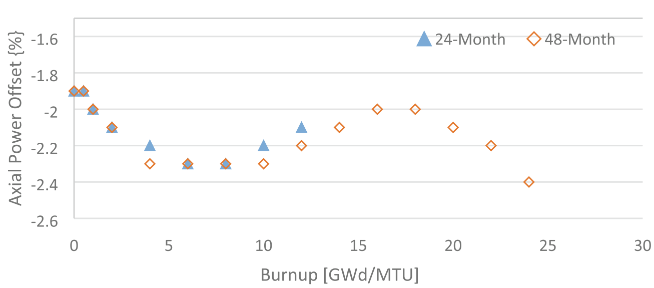

Fig. 5. Axial offset factors along with the burnup.

1146 ppm. This increase in boron content may contribute to an increase in Zircaloy corrosion and oxidation. Despite the substantial increase in burnable poison, the boric acid concentration in the RCS remains below standard PWR limits as shown in Table 2; however, this was offset by the addition of LBP within some fuel rods. The significant increase in boron concentration shown in Fig. 8 suggests possible design limitations in higher enriched cores; although, the effect of an increase in boron concentration can be diminished by increasing core LBP concentration. The equilibrium LBP was not adjusted for the equilibrium cycle 48-month core but was adjusted for the first cycle fresh fuel core. Although the boron content in the reactor remains below the standard limit of 2,000 ppm, there are still significant safety concerns that may arise from an increase in boron concentration: these being an increase in tritium production and higher levels of crud deposition.

3.2.3. *Fuel cycle effects*

In addition to reactivity changes, higher enriched fuel accounts for a significant change in fuel depletion characteristics. One such change is the prominent increase in fission product poison content in fuel rods. Figs. 9 and 10 show changes in Sm-149 and Xe-135 content in both cores. The Xe-135 and Sm-149 content was found to increase by a maximum of 35% and 129%, respectively. Being that the 48-month core experienced no change in I-135 and a slight reduction in Pm-149, the rise in their daughter nuclei may result from an overall reduction in their loss mechanisms. Because of the decrease in core-averaged thermal flux shown in Fig. 6, the rate of removal of Xe-135 and Sm-149 is reduced. The effects of this trend are less significant for Xe-135 because the reduction of Pu-239 in higher enriched fuel causes a reduction in Xe-135 fission yields (IAEA. (n.d.). Fission product yields. Retrieved August 15, 2020).

The reactor operational history is important due to its impact on characteristics of the fission products and the amount of decay heat produced. The overall concentration of radioactive fission products after reactor shutdown is a function of reactor burnup and power history. Increasing decay heat extends the time for a reactor to reach the "minimum heat" necessary for refueling to begin. This decay heat is roughly approximated for a constant power operating history by the Wigner-Way formula shown below:

$$\frac{P(t)}{P_0} = 6.85 \times 10^{-3}\left[t^{-0.2} - (t_o + t)^{-0.2}\right] \tag{2}$$

where $P(t)/P_0$ is the ratio of decay heat to the constant operating power, t is time after shutdown in days, and t_o is time of reactor operation in days (Pond and Matos, 1996). Under the assumption that the time to reach the decay heat limit is the critical path in a refueling

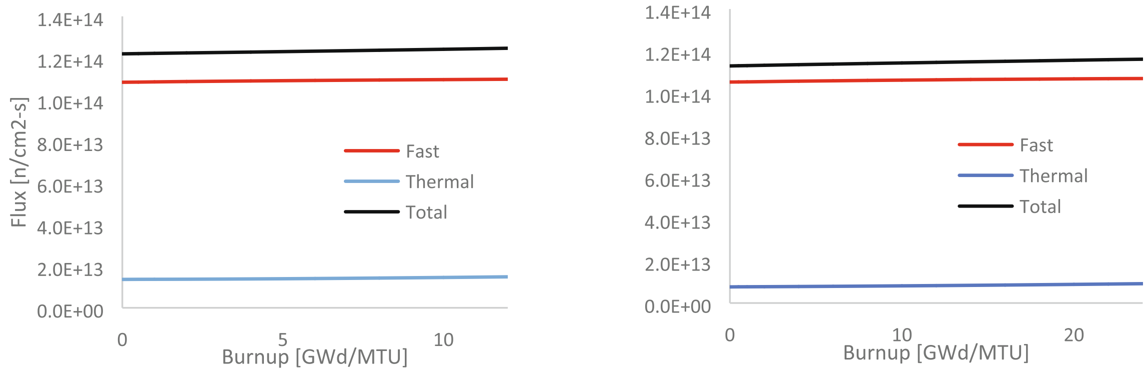

(a) 24-month Core (b) 48-month Core

Fig. 6. Core averaged flux along with burnup for different cycle length cores.

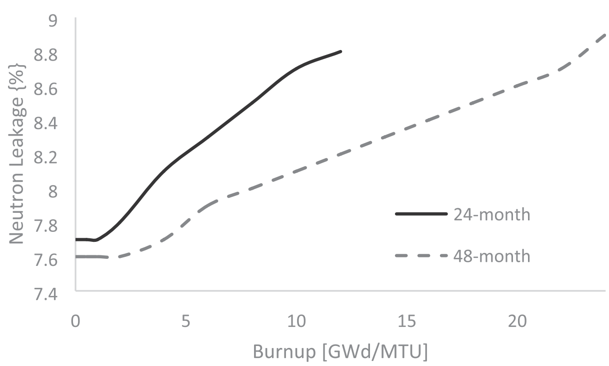

Fig. 7. Neutron leakage rate along with burnup.

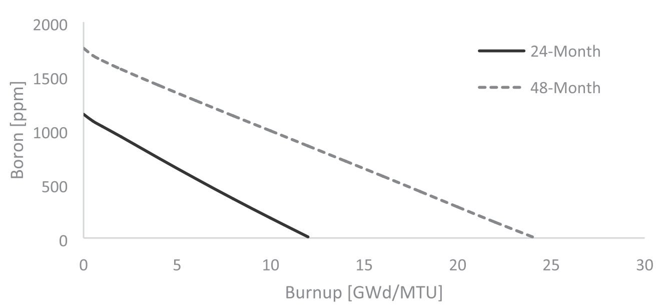

Fig. 8. Boron letdown curves.

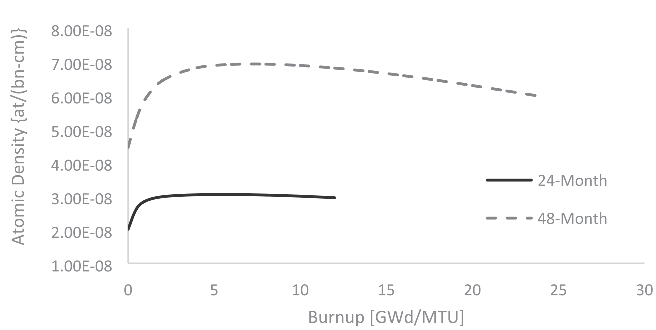

Fig. 9. Samarium content along with the burnup.

outage, the NuScale SMR has an active pool cooling operation of 3 days under normal operation (U. S. NRC., 2009). Fig. 11 shows the decay heat effect of different fuel cycle length based on Eq. (2) where each blue

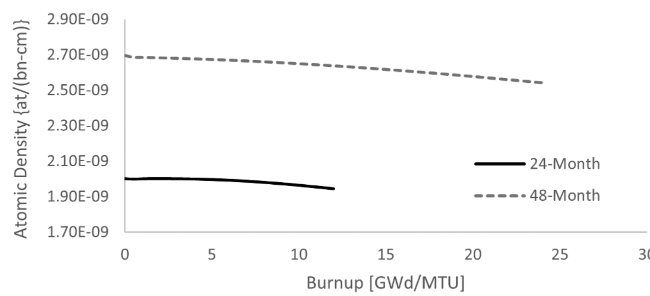

Fig. 10. Xenon content along with the burnup.

curve represents a cycle time measured in years and yellow line represents the decay heat level of the NuScale core after 3 days cooling after shutdown. As shown in the figure, if the fuel cycle length is doubled from two years to four years, the resulting refueling time would extend by roughly one full day. The effect of decay heat would reduce a four-year capacity factor by approximately 0.1%. Ultimately, although there is a considerable increase in refueling time, the overall effect on reactor capacity factor is not enough to significantly affect plant economics.

3.3. Thermal hydraulic analysis results

Despite the increase in average fuel burnup for an equilibrium fuel cycle, the 48-month reactor experiences a slightly lower average fuel temperature as indicated in Fig. 12. This decrease in fuel temperature can be attributed to a reduction in core-averaged flux as shown in Fig. 6.

Although producing the same power at a lower average fuel temperature may be a positive safety implication, the higher GPF of the 48-month reactor results in an increased peak fuel cladding temperature, which is a significant implication for determining plant safety criteria. Because peak cladding temperature was not an output in the SIMULATE code, values for peak cladding temperature were approximated using average fuel temperature, GPF, and moderator temperature; these values were calculated using a standard conduction/convection heat transfer model with 1-D cylindrical geometry. Eq. (3) shows the standard analytical equation for calculating heat transfer (Penoncello, 2018).

$$\overline{q'} = \frac{\overline{T}_{c,i} - \overline{T}_{\infty}}{R_t} \tag{3}$$

where $\overline{q'}$ represents the average thermal power $\left(\frac{W}{m}\right)$, $\overline{T}_{c,i,max}$ is the average temperature (k) at the inner radius of the fuel cladding, $\overline{T}_{\infty}$ is the average temperature of the coolant, and R_t is the total thermal

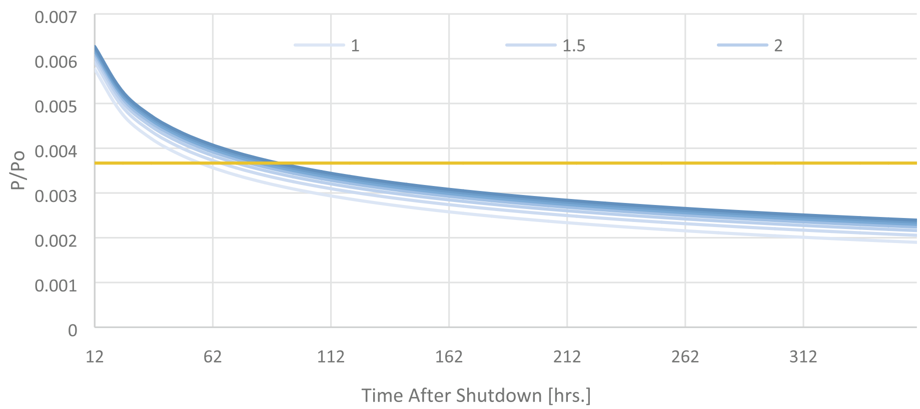

Fig. 11. Decay heat effect on shutdown time with different fuel cycle length in years.

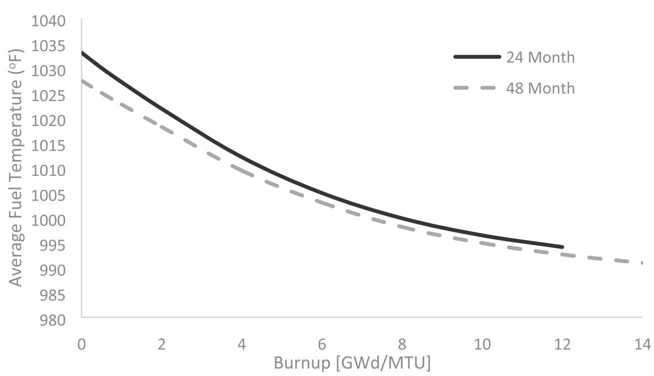

Fig. 12. Average fuel rod temperature along with the burnup.

resistance $\left(\frac{m*k}{W}\right)$ from the inner cladding to the coolant. Using the thermal circuit method (Penoncello, 2018), the total thermal resistance equation from the inner cladding to the coolant is determined to be that shown by Eq. (4).

$$R_t = \frac{1}{2\pi}\left[\frac{ln(R_{c,o}/R_{c,i})}{k_c} + \frac{1}{R_{c,o}h_{\ mod}}\right] \quad (4)$$

where $R_{c,i}$ and $R_{c,o}$ are the inner and outer radii (m) respectively, k_c is the thermal conductivity $\left(\frac{W}{k*m}\right)$ of the cladding, and $h_{\ mod}$ $\left(\frac{W}{k*m^2}\right)$ is the heat transfer coefficient associated with the coolant flow. By substituting Eq. (4) into Eq. (3), a formula for the average inner cladding temperature may be found as shown in Eq. (5).

$$\overline{T}_{c,i} = \frac{\overline{q'}}{2\pi}\left[\frac{ln(R_{c,o}/R_{c,i})}{k_c} + \frac{1}{R_{c,o}h_{\ mod}}\right] + T_\infty \quad (5)$$

To find the local cladding temperature, the average power can be multiplied by the power peaking factor or hot channel factor, $(F(z))$, to solve for the localized power. By multiplying the core power by the GPF, $(F(z))_{GPF}$, throughout a reactor cycle, the maximum cladding temperature may be approximated as shown by Eq. (6).

$$T_{c,i,max} = \frac{\overline{q'}(F(z))_{GPF}}{2\pi}\left[\frac{ln(R_{c,o}/R_{c,i})}{k_c} + \frac{1}{R_{c,o}h_{\ mod}}\right] + T_\infty \quad (6)$$

To find the heat transfer coefficient of the moderator, the Eq. (7) may be used (Penoncello, 2018).

$$h_{\ mod} = \frac{Nu_\infty k_c}{D_c} \quad (7)$$

where Nu_∞ is the Nusselt number under fully-developed conditions and D_c is the hydraulic diameter of the cladding (m). The Nusselt number may be approximated using Eq. (8) (Todreas and Kazimi, 2012).

$$Nu_\infty = \psi(Nu_\infty)_{C.L.} \quad (8)$$

where $(Nu_\infty)_{C.L.}$ is the Nusselt number for a circular tube found using the Dittus-Boelter equation (Eq. (9)), and ψ is a correction factor which adjusts for the lattice geometry of the fuel pins found using Eq. (10) (Todreas and Kazimi, 2012).

$$Nu_\infty = 0.023Re_d^{0.8}Pr^{0.4} \quad (9)$$

$$\psi = 0.9217 + 0.1478\left(\frac{P}{D}\right) - 0.1130e^{-7\left[\left(\frac{P}{D}\right)-1\right]} \text{ for } \left(1.05 \leqslant \frac{P}{D} \leqslant 1.9\right) \quad (10)$$

where Re_d is the Reynolds number, Pr is the Prandtl number, and $\frac{P}{D}$ is the pitch-to-diameter ratio. Lastly, to solve for the maximum cladding temperature, the Reynolds Number must be found using Eq. (11) (Penoncello, 2018).

$$Re_d = \frac{\rho u_m D_c}{\mu} \quad (11)$$

where ρ is the coolant density, u_m is the coolant velocity, and μ is the coolant viscosity. Though the peak cladding temperature is higher for the 48-month reactor than that of the 24-month reactor, the difference between the maximum temperature is marginal and unlikely to seriously affect reactor safety. However, the long term exposure to higher temperatures could be a concern regarding increased corrosion and crud deposit rates in certain regions of the reactor. Fig. 13 shows the predictions of peak cladding temperature during operation with the simple analytic model outline above, which indicates the peak cladding temperature slightly increased at the beginning of the extended cycle core, but it decreases with the burnup and falls within the safety restraints throughout the cycle.

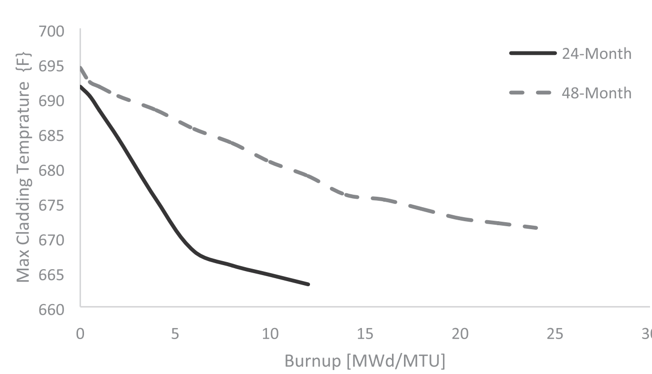

Fig. 13. Peak cladding temperature along with the burnup.

3.4. Material analysis results

The zirconium alloys typically used for cladding and fuel assembly components have excellent corrosion and radiation resistant properties (Choi and Kim, 2013). Although there is no significant change in flux caused by increasing fuel enrichment, extending cycle time will drastically change the design criteria of fuel assemblies. Due to the anisotropic nature of zirconium and zirconium alloys, the increased fluence of cladding material due to prolonged exposure may lead to increased irradiation growth. Deformation from increased neutron fluence adds stress and increases likelihood of failure (Choi and Kim, 2013). Irradiation growth of zirconium is dependent on composition, grain size, level of cold-working or annealing, and temperature (Choi and Kim, 2013; Adamson et al., 2019). Core components are typically constructed from Zircaloy-2, Zircaloy-4, Zr-2.5Nb, ZIRLO, M4, and/or M5. M5 was chosen for NuScale's cladding while Zr-4 was chosen for assembly spacer grids and control rod assembly (CRA) guide tubes. M5 is an advanced zirconium alloy which takes advantage of the ability of high sulfur concentrations to reduce irradiation creep and growth (Adamson et al., 2019). This aspect of the design makes increasing core burnup an attainable goal. The increased fluence of M5 zirconium alloy cladding due to increased burnup can be estimated using approximated conversion factors (Adamson et al., 2019):

$$50\,\mathrm{GWd/MT} = 1 \times 10^{26}\,\mathrm{n/m^2}(\mathrm{E} > 1\,\mathrm{MeV}) = 15.4\,\mathrm{dpa} \tag{12}$$

where the unit dpa, or displacement per atom, is used as a measure of material damage due to neutron exposure. Using this approach, the NuScale SMR will achieve an approximate maximum fluence of 7.20×10^{25}, 1.08×10^{26}, and $1.44 \times 10^{26}\mathrm{n/m^2}$ for cycle times of 2, 3, and 4 years respectively. The corresponding damage for M5 cladding will then be 11.1, 16.6, and 22.2 dpa for cycle times of 2, 3, and 4 years respectively. Since an assembly may be present in the reactor for up to three cycles, the lifetime damage for cladding in 4 year cycle reactor will experience 66.5 dpa. With increased fluence, there is expected to be additional cladding creep; this creep can be approximated using the Eq. (13), a relationship determined from empirical M5 test data (Adamson et al., 2019).

$$\varepsilon = 0.126F - 0.0626 \tag{13}$$

where ε represents the percent strain due to creep and F represents the neutron fluence in $10^{25}\mathrm{n/m^2}$. Plugging the fluence values into Eq. (13) results in creep strains of 0.84, 1.30, and 1.75 percent for the respective cycle periods of 2, 3, and 4 years. This additional creep strain, coupled with radiation embrittlement, increases the risk of fuel rod failure.

Assuming increasing enrichment to HALEU levels has a negligible effect on RPV flux and temperature, ferritic material is expected to corrode slightly faster at higher enrichments. This suggests an RPV will reach its toughness limits earlier than it would when using fuels below 5% enrichment resulting in a shorter overall reactor lifetime. For example, if a reactor with a 60 year lifetime and 24 month refueling cycle at 95% capacity factor extended its cycle period by 24 additional months, the new capacity factor would be 97.5%. This cycle extended reactor would reach roughly the same lifetime fluence in 58.5 years. However, a precise RPV fluence calculation is difficult to estimate and requires complex computer simulations because increasing fuel enrichment affects core neutronics, thermal-hydraulics, and material properties that would all influence neutron flux levels for the RPV (Power, 2016). For these reasons, as well as a lack of empirical evidence, it is difficult to estimate how much a reactor's lifetime would be reduced as a result of increasing fuel enrichment.

3.5. Economic analysis results

For the economic analysis, the key input parameter is the average LCOE of NuScale's SMR design, which is reported to be approximately 86 $/MWh in Ref. (U.S. NRC., 2012). It is important to note that this parameter may be subject to change as this design moves forward towards implementation. Following the discussion provided to Section 2.4, a preliminary economic analysis of the case study was performed, and the results of the analysis were covered in greater detail in Ref. (Carlson et al., 2020). Some important findings are repeated in this paper for a complete discussion. The change in LCOE due to increased enrichment may only be considered economically viable if the increase in fuel costs for a single cycle are less than the benefits derived from increasing the fuel cycle length. Fig. 14 illustrates this concept by displaying the estimated LCOE for product enrichments of 5–20 w/o with cycle lengths of 2.5, 3, 3.5, and 4 years with a fixed tails enrichment of 0.2 w/o. This only provides an assessment based on purely economic factors and does not account for the potential technical limitations of NuScale's SMR design.

As shown in Fig. 14**,** the lowest theoretical LCOE appears for the case with a four-year cycle at 5 w/o; however, this design is unachievable at that enrichment without reducing power or significantly changing the design of the reactor. Because of this, Fig. 14 can best be interpreted as a way of determining the economic viability of a design after finding the optimal cycle length at full power for fuel at HALEU level enrichments. If this optimized enrichment falls to the left of the intersection of the red line and the corresponding cycle length LCOE curve, the design would be economically viable compared to the original design. If this value falls to the right, however, the HALEU fuel design would be economically detrimental. To achieve cycle lengths of 2.5, 3, 3.5, and 4 years, the corresponding core-averaged fresh fuel enrichments must remain below 5.4, 6.6, 7.8 and 9.0 w/o respectively. By extrapolating this trend, it is revealed that the minimum economically viable cycle length for an average fuel enrichment of 20 w/o is 8.6 years. To verify the economic benefits of extending cycle length for NuScale's SMR design, the corresponding optimal fuel enrichment is required to achieve a desired fuel cycle length and must be obtained through an in-depth reactor analysis simulation.

Based on the LCOE data shown in Fig. 14, the HALEU SMR design described above is estimated to operate at an LCOE of 84.8 $/MWh, or 1.23 $/MWh less than that of NuScale's 24-month design. By assuming a linear reactivity model (LRM) (Parks, 1989), a relationship for enrichment and cycle length was established by comparing NuScale data to the simulated SMR 48-month cycle results. Fig. 15 illustrates this relationship. By interpolating the LRM results, the optimal core loading enrichments for 30, 36, and 42-month cycles were found to be 5.21, 6.26, and 7.30 w/o while their corresponding LCOEs were 85.5, 85.2, and 84.9 $/MWh respectively. The red and yellow error bars represent errors corresponding to input price data uncertainties of 1% and 5% respectively. The trends observed in Fig. 15 suggest that the improvement in LCOE from the original 24-month cycle due to increased enrichment

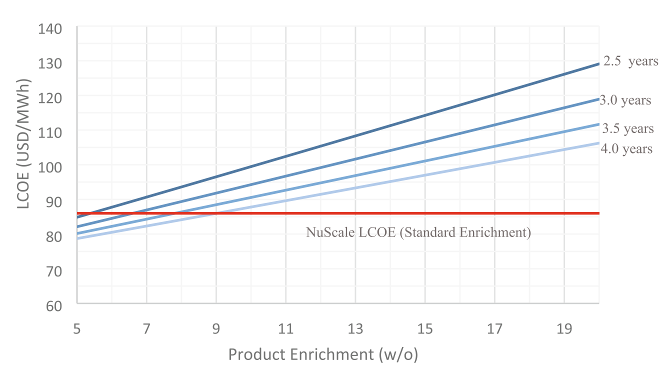

Fig. 14. Projected LCOE of target enrichments and cycle lengths (Turnbull, et al., 2020). Note the red line refers to the estimated LCOE for NuScale's current SMR design. (For interpretation of the references to colour in this figure legend, the reader is referred to the web version of this article.)

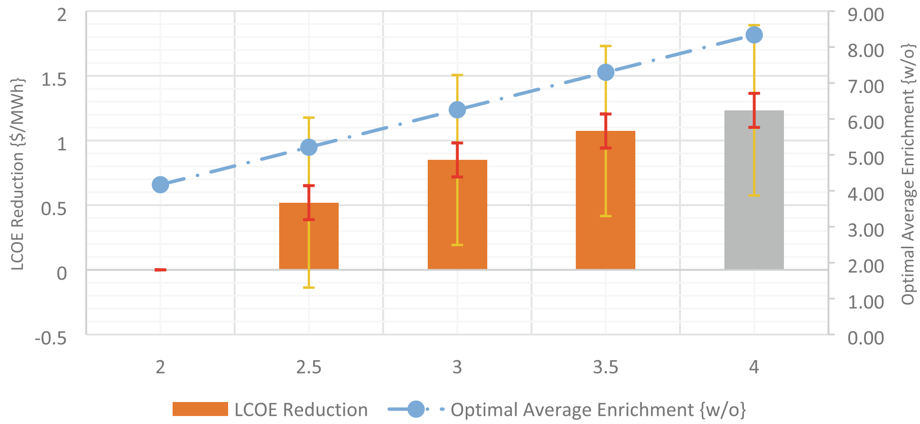

Fig. 15. Optimized enrichment and LCOE for SMR with extended cycle length (Turnbull, et al., 2020).

becomes less significant as cycle time increases. The approximated data points from 2.5 to 3.5 years were derived using an LRM; because of this, the corresponding data are not as well-defined as those derived from a more rigorous physics model (like the model used to simulate the 4-year case).

With a power output of 45 MWe, the yearly savings for one 48-month cycle reactor using HALEU fuel is estimated to be $486,000. With a NuScale power plant of 12 modules, the total yearly savings are expected to be roughly $5,840,000. Therefore, it is shown that increasing the fuel enrichment to extend cycle length to 48 months may greatly increase the economic efficiency of an SMR. This estimate ignores such factors as lack of current HALEU manufacturing infrastructure and increased fuel transport costs which may diminish the economic benefits of HALEU fuels in the short-term.

4. Conclusion

The research carried out in this paper aimed to identify the most significant effects on reactor performance that may result from increasing fuel enrichment beyond its current legal limit. Using the NuScale's 160 MWth reactor as a model reactor, a case study was performed to provide a better understanding of how certain parameters may change in a reactor with longer cycle times, higher fuel burnup, and higher fuel enrichment. Many of these parameters were tested against known operating limits and safety constraints to determine the feasibility of operating a reactor with HALEU fuel.

To determine the feasibility of these reactors, many implications to reactor performance were identified and their corresponding theories were discussed. These implications were categorized by neutronics, thermal-hydraulics and safety, material, and economic considerations. Within the neutronics category, five considerations were discussed: global peaking factor, reactivity coefficients, burnable poison concentration, flux and fission product concentration, and fuel cycle. While core-averaged power is expected to stay the same for a higher enriched, longer cycle reactor, the global peaking factor is expected to increase. Another key concern is that both the moderator and fuel temperature reactivity feedback coefficients will become less negative. Also discussed, was the possibility of higher boric acid and/or LBP concentrations. Additionally, the concentrations of key fission product poison isotopes like ^{135}Xe and ^{149}Sm are expected to change with increased fuel enrichment, with ^{135}Xe expected to rise sharply. The thermal flux of the reactor was also expected to decrease. As for the fuel cycle, HALEU fuel is expected to have more benefit than lower enriched fuel. For example, HALEU fuel may lead to an overall reduction in DU, LLW, HLW, land-usage, carbon output, and actinide concentration in SNF. On the other hand, there is a slightly higher expected increase in water usage. While there is no significant impact on core power from higher enriched fuel, the expected increased boron concentration may lead to an increase in crud depositing and boron crystallization which may lead to increased occurrences of AOA and reactivity excursion events which could be a serious concern regarding power distribution. One negative aspect of HALEU fuel mentioned was the issue of the transportation of higher enriched fuel which is a major proliferation concern. As for material concerns, increased neutron fluence can limit RPV life, greater power distribution can lead to increased cladding creep and fuel swelling, prolonged cycle times can lead to increased crud deposition, and higher burnup leads to HBS formation and RIP. Lastly, reactor LCOE benefits from reduced fuel supply and increased capacity but suffers from higher fuel costs.

Operating at a 48-month cycle with an optimized average fuel enrichment of 8.34 w/o, the maximum equilibrium cycle GPF was found to exceed that of the 24-month design by only 0.04. Correspondingly, the maximum peak cladding temperature deviated modestly from that of the 24-month cycle, while the average fuel temperature remained closely aligned as a function of burnup. Additionally, the maximum axial offset value was determined to be −2.4% which falls well within the safety constraints listed in Table 2; although the trend suggests that axial offset may become a concern with increasing burnup, which may act as a limiting factor for higher fuel enrichments. Likewise, while boron concentration managed to remain below the given safety constraint of 2000 ppm, there was a significant increase in boron content, suggesting that higher enrichments may warrant the use of increased LBP in fuel to reach higher burnup values. Moreover, the decrease in core-averaged flux and increase in neutron leakage and fission product poison concentration may warrant consideration of fuel rod design modifications and core layout for more optimized fuel utilization. Regarding the mechanical aspect, cladding creep was roughly calculated to grow approximately from 0.84% to 1.75% from 2 to 4 year cycle times respectively. Lastly, the economic study shows that increasing enrichment to HALEU levels may be a very promising method to improve the economic efficiency of SMR and micro-reactor designs. It is worth mentioning that the plant's maintenance outages should also be extended to 48 months for these results to hold true.

Although the tested implications remain within the safety constraints for a 48-month core design, there are still many implications that must be investigated. For one, it is important to study how increasing enrichment effects levels of high-level waste and how the isotopic composition of that waste may change. It is especially important to determine the plutonium content of spent fuel, as this may affect its proliferation resistance. Additionally, expected changes in RPV material irradiation and corrosion must be investigated as a higher capacity factor may be offset by the reduction in core-averaged flux as shown in Fig. 7. Also, the increase in cladding material creep, growth, corrosion, crud deposition, and radiation embrittlement must be tested for increased burnup and cycle time. Similarly, from a fuel standpoint, cracking and HBS development must be considered when analyzing changes due to increased burnup.

Since the results of the case study were mainly solved using standard reactor analysis codes, the feasibility of increasing fuel enrichment and cycle length must be investigated further with more in-depth reactor analysis methods. Despite this, the results from this case study show that increasing fuel enrichment beyond 5 w/o to extend cycle length may be both attainable and cost effective. In fact, extending cycle length to 48-months may reduce the LCOE by 1.23 $/MWh while remaining within the limits of all investigated safety constraints; however, parameters such as boron concentration and axial flux or power offset may act as limiting factors as fuels are enriched further and cycle lengths are extended. In general, it is shown that while there are some causes for concern, a PWR type SMR may realistically be able to extend its fuel enrichment past the current legal limit and remain within its pre-established safety constraints.

CRediT authorship contribution statement

Liam Carlson: Data curation, Formal analysis, Investigation, Resources, Software, Visualization, Writing – original draft. **James Miller:** Methodology, Supervision, Investigation, Resources, Writing – review & editing. **Zeyun Wu:** Conceptualization, Methodology, Project administration, Supervision, Investigation, Resources, Writing – review & editing.

Declaration of Competing Interest

The authors declare that they have no known competing financial interests or personal relationships that could have appeared to influence the work reported in this paper.

Acknowledgements

We are grateful to the computational efforts performed on a SMR design project by a senior design team at Virginia Commonwealth University. The first author was part of the design team. Other team members include Brendan Fisher, Michael Cartwright, and Caleb Taylor.

References

Kirshenberg, S., et al. (2017). Small Modular Reactors: Adding to Resilience at Federal Facilities. Technical report, Kutak Rock LLP & Scully Capital Services Inc.

WNA. (2020). *Small Nuclear Power Reactors*. Retrieved August 10, 2020, from https://www.world-nuclear.org/information-library/nuclear-fuel-cycle/nuclear-power-reactors/small-nuclear-power-reactors.aspx.

McGinnis, E. (2019). The BIG Potential for Nuclear Microreactors. Retrieved May 21, 2020, from ttps://www.energy.gov/ne/articles/big-potential-nuclear-microreactors.

Charles, C. (2018). Micro-Reactors Could Power Remote Military Bases within a Decade. Retrieved May 22, 2020, from https://www.nei.org/news/2018/micro-reactors-power-remote-military-bases.

Locatelli, G., Bingham, C., Mancini, M., 2014. Small modular reactors: A comprehensive overview of their economics and strategic aspects. Progress in Nuclear Energy 73, 75–85. https://doi.org/10.1016/j.pnucene.2014.01.010.

Prasad, S., Abdulla, A., Morgan, M.G., Azevedo, I.L., 2015. Nonproliferation improvements and challenges presented by small modular reactors. Progress in Nuclear Energy 80, 102–109. https://doi.org/10.1016/j.pnucene.2014.11.023.

Moormann, R., Kemp, R.S., Li, J.u., 2018. Caution Is Needed in Operating and Managing the Waste of New Pebble-Bed Nuclear Reactors. Joule 2 (10), 1911–1914. https://doi.org/10.1016/j.joule.2018.07.024.

Wade, D.C., Fujita, E.K., 1989. Trends vs. reactor size of passive reactivity shutdown and control performance. Nuclear Science and Engineering 103, 182–195. https://doi.org/10.13182/NSE89-6.

U.S. NRC. (2012). NuScale Plant Design Overview. Technical report, retrieved June 4, 2020, from https://www.nrc.gov/docs/ML1221/ML12216A392.pdf.

Nagley, S. (2020). HA-LEU Supply (Enrichment, De-conversion, Fuel Fab & Transportation). Technical report, BWXT. Retrieved May 21, 2020 from https://gain.inl.gov/HALEU_Webinar_Presentations/12-Nagley,BWXT-28Apr2020.pdf.

Eidelpes, E.F., et al., 2019. UO_2 HALEU Transportation Package Evaluation and Recommendations. Technical report, INL. https://doi.org/10.2172/1578279.

U.s. doe. Status of Advanced Reactor Demonstration Programs. Technical report, DOE Retrieved May 21 2020 ARDP_Status_for_HALEU_Workshop, Rev1-28Apr2020.pdf. 2020 from.

Moe, W.L., 2019. Key Regulatory Issues in Nuclear Micro-Reactor Transport and Siting. Technical report, INL. https://doi.org/10.2172/1616515.

Collin, B.P., 2016. GEN-IV Benchmarking of TRISO Fuel Performance Models under accident conditions modeling input data. Technical report, INL. https://doi.org/10.2172/1389200.

Wilson, T.L., Moore, E.E., Adorno Lopes, D., Kocevski, V., Sooby Wood, E., White, J.T., Nelson, A.T., McMurray, J.W., Middleburg, S.C., Xu, P., Besmann, T.M., 2018. Uranium nitride-silicide advanced nuclear fuel: Higher efficiency and greater safety. Advances in Applied Ceramics 117 (sup1), s76–s81. https://doi.org/10.1080/17436753.2018.1521607.

Lewis, E.E., 2008. Fundamentals of Nuclear Reactor Physics. Elsevier, Burlington, MA.

Wu, Z., et al., 2016. A Core Design for a Small Modular Boiling Water Reactor with Long-Life Core. Nuclear Technology 193, 364–374. https://doi.org/10.13182/NT15-58.

Wu, Z., Williams, R.E., Rowe, J.M., Newton, T.H., O'Kelly, S., 2017. Neutronics and Safety Studies on a Research Reactor Concept for an Advanced Neutron Source. Nuclear Technology 199 (1), 67–82. https://doi.org/10.1080/00295450.2017.1335146.

U.S. NRC. Acceptance Criteria for Emergency Core Cooling Systems for Light-Water Nuclear Power Reactors. US Code of Federal Regulations 2012 Nuclear Regulatory Commission, Rockville, MD.

Hirai, M., 1990. Thermal diffusivity of UO2-GD2O3 Pellets. Journal of Nuclear Materials 173 (3), 247–254. https://doi.org/10.1016/0022-3115(90)90392-z.

Burns, J.R., Hernandez, R., Terrani, K.A., Nelson, A.T., Brown, N.R., 2020. Reactor and fuel cycle performance of light water reactor fuel with ^{235}U enrichments above 5%. Annals of Nuclear Energy 142, 107423. https://doi.org/10.1016/j.anucene.2020.107423.

U.S. NRC. (2017). Low-Level Waste. Retrieved August 10, 2020 from https://www.nrc.gov/waste/low-level-waste.html.

D.E. Beller R.A. Krakowski Burnup Dependence of Proliferation Attributes of Plutonium from Spent LWR Fuel (Rep.). LA-UR-99-751 1999 Los Alamos, NM.

Li, S., Yang, D., Zhang, T., Liu, X., 2019. A Combined Method for Predicting the Boron Deposited Mass and the CIPS Risk. Science and Technology of Nuclear Installations 2019, 1–8. https://doi.org/10.1155/2019/9537421.

D'Auria, F., 2017. Thermal hydraulics in water-cooled nuclear reactors. Woodhead Publishing, Elsevier, Amsterdam.

Odette, R., Zinkle, S., 2019. Structural alloys for nuclear energy applications. Elsevier, Amsterdam.

U.S. NRC. (2018). Backgrounder on Steam Generator Tube Issues. Retrieved August 10, 2020 from https://www.nrc.gov/reading-rm/doc-collections/fact-sheets/steam-gen.html.

U.S. NRC. (2019). Standard Technical Specifications – Operating and New Reactors – Current Versions. Retrieved August 10, 2020 from https://www.nrc.gov/reactors/operating/licensing/techspecs/current-approved-sts.html.

U.S. NRC. (2012).Standard Technical Specifications Westinghouse Plants Revision 4.0. Technical report. Retrieved August 10, 2020 from https://www.nrc.gov/docs/ML1210/ML12100A222.pdf.

U.S. NRC. (2020). Standard Technical Specifications Westinghouse Advanced Passive 1000 (AP1000) Plants. Technical report. Retrieved August 10, 2020 from https://www.nrc.gov/docs/ML1611/ML16110A277.pdf.

U.S. NRC. (2020). Standard Technical Specifications Babcock and Wilcox Plants Revision 4.0. Technical report. Retrieved August 10, 2020 from: https://www.nrc.gov/docs/ML1210/ML12100A177.pdf.

R.E. Ginna Nuclear Power Plant. (2018). Core Operating Limits Report (COLR) Cycle 41, Technical report. Retrieved August 10, 2020 from https://www.nrc.gov/docs/ML1833/ML18331A165.pdf.

U.S. NRC. (2007). NO-1 Cycle 21 Core Operating Limits Report (COLR). Technical report. Retrieved August 10, 2020 from https://www.nrc.gov/docs/ML0712/ML071240117.pdf.

U.S. NRC. (2010). Pressurized Water Reactor B&W Technology Crosstraining Course Manual Chapter 22.0 Plant Operating Limits (Manual Chapter). Retrieved August 10, 2020 from https://www.nrc.gov/docs/ML1122/ML11221A355.pdf.

U.S. NRC. (2011). Core Operating Limits Report (COLR) for Prairie Island Nuclear Generating Plant IPINGP) Unit I, Cycle 27. Technical report. Retrieved August 10, 2020 from https://www.nrc.gov/docs/ML1115/ML111540118.pdf.

U.S. NRC (2019). Appendix H to Part 50—Reactor Vessel Material Surveillance Program Requirements. Technical report. Retrieved August 10, 2020 from https://www.nrc.gov/reading-rm/doc-collections/cfr/part050/part050-apph.html.

U.S. NRC (2019). Appendix G to Part 50—Fracture Toughness Requirements. Technical report. Retrieved August 10, 2020 from https://www.nrc.gov/reading-rm/doc-collections/cfr/part050/part050-appg.html.

Adamson, R.B., Coleman, C.E., Griffiths, M., 2019. Irradiation creep and growth of zirconium alloys: A critical review. Journal of Nuclear Materials 521, 167–244. https://doi.org/10.1016/j.jnucmat.2019.04.021.

Chan, K.S., 1996. A micromechanical model for predicting hydride embrittlement in nuclear fuel cladding material. Journal of Nuclear Materials 227 (3), 220–236. https://doi.org/10.1016/0022-3115(95)00160-3.

Rest, J., Cooper, M.W.D., Spino, J., Turnbull, J.A., Van Uffelen, P., Walker, C.T., 2019. Fission gas release from UO_2 nuclear fuel: A review. Journal of Nuclear Materials 513, 310–345. https://doi.org/10.1016/j.jnucmat.2018.08.019.

Une, K., Kashibe, S., Takagi, A., 2006. Fission Gas Release Behavior from High Burnup UO2 Fuels under Rapid Heating Conditions. Journal of Nuclear Science and Technology 43 (9), 1161–1171. https://doi.org/10.3327/jnst.43.1161.

Machiels, A.J., Rashid, J.Y.R., Lyon, W.F., Sunderland, D.J., 2017. Characterization of end-of-life rod internal pressure in PWR fuel. Nuclear Engineering and Design 324, 250–259. https://doi.org/10.1016/j.nucengdes.2017.09.002.

Kim, J.-S., Hong, J.-D., Yang, Y.-S., Kook, D.-H., 2017. Rod internal pressure of spent nuclear fuel and its effects on cladding degradation during dry storage. Journal of Nuclear Materials 492, 253–259. https://doi.org/10.1016/j.jnucmat.2017.05.047.

Kim, JUSEONG, Yoon, HAKKYU, Kook, DONGHAK, Kim, YONGSOO, 2013. A Study on the Initial Characteristics of Domestic Spent Nuclear Fuels For Long Term Dry Storage. Nuclear Engineering and Technology 45 (3), 377–384.

Turnbull, J. A., et al. (n.d.). A review of fission gas release data within the NEA/IAEA IFPE database. Technical report, NEA. Retrieved August 10, 2020 from https://www.oecd-nea.org/science/wprs/fuel/fgr-cad-2k-m1.pdf.

Gussev, M.N., Byun, T.S., Yamamoto, Y., Maloy, S.A., Terrani, K.A., 2015. In-situ tube burst testing and high-temperature deformation behavior of candidate materials for accident tolerant fuel cladding. Journal of Nuclear Materials 466, 417–425. https://doi.org/10.1016/j.jnucmat.2015.08.030.

Pimentel, F. (2019). The Economic Benefits and Challenges with Utilizing Increased Enrichment and Fuel Burnup for Light-Water Reactors. Technical report, NEI. Retrieved May 21, 2020 from https://www.nei.org/CorporateSite/media/filefolder/resources/reports-and-briefs/NEI-White-Paper-The-Economic-Benefits-and-Challenges-with-Utilizing-Increased-Enrichment-and-Fuel-Burnup-for-LWR.pdf.

Carlson, L., Wu, Z., Olson, J., Liu, L.(., Zucchetti, 2020. An Economic Cost Assessment on HALEU Fuels for Small Modular Reactors. Science and Technology of Nuclear Installations 2020, 1–6. https://doi.org/10.1155/2020/8815715.

Studsvik, Reactor Design and Performance Optimization www.studsvik.com/our-solutions/nuclear-fuel–reactor-performance-optimisation/software-products/reactor-design-and-performance-optimization/ 2009 Retrieved May 21, 2020 from.

Welter, K., 2010. NuScale Technology Overview. Retrieved May 21, 2020 from. https://www.nrc.gov/docs/ML1034/ML103470495.pdf.

IAEA. (n.d.). Fission product yields. Retrieved August 15, 2020 from https://www-nds.iaea.org/wimsd/fpyield.htm.

R.B. Pond J.E. Matos Nuclear Mass Inventory, Photon Dose Rate and Thermal Decay Heat of Spent Research Reactor Fuel Assemblies Technical report Rev. 1 1996 Argonne National Laboratory Argonne, IL 6 9.

U. S. NRC. (2009). Refueling Operations Report for NuScale Power Module. Technical report. Retrieved June 12, 2020 from https://www.nrc.gov/docs/ML0908/ML090850080.pdf.

S.G. Penoncello Thermal Energy Systems: Design and Analysis 2nd Ed. 2018 Taylor & Francis CRC Press.

N.E. Todreas M.S. Kazimi Nuclear Systems vol. 1 2nd ed. 2012 Taylor & Francis CRC Press.

Choi, S.I., Kim, J.H., 2013. Radiation-Induced Dislocation and Growth Behavior of Zirconium and Zirconium Alloys – A Review. Nuclear Engineering and Technology 45 (3), 385–392. https://doi.org/10.5516/net.07.2013.035.

NuScale Power (2016). Fluence Calculation Methodology and Results (Rep.), Corvallis, OR. Retrieved August 10, 2020 from https://www.nrc.gov/docs/ML1700/ML17005A116.pdf.

Parks, G., 1989. A piecewise linear reactivity fuel-cycle model. Annals of Nuclear Energy 16 (8), 417–422. https://doi.org/10.1016/0306-4549(89)90104-7.